

Progress towards robotic in-situ dating of martian sediments using optically stimulated luminescence

Regina Kalchgruber^{a,*}, Michael W. Blair^{a,c}, Stephen W.S. McKeever^a,
Eric R. Benton^a, Dennis K. Reust^b

^aDepartment of Physics, Oklahoma State University, 145 Physical Sciences II, Stillwater, OK 74078, USA

^bNomadics Inc., 1024 S. Innovation Way, Stillwater, OK 74074, USA

^cLos Alamos National Laboratory, Earth and Environmental Sciences Division, EES 2 MS J495, Los Alamos, NM 87545, USA

Received 29 December 2006; received in revised form 15 May 2007; accepted 13 September 2007

Available online 21 September 2007

Abstract

Recent exploratory efforts to reveal the evolution and the climatic history of Mars have shown that the planet is still active. The surface of Mars has been, and continues to be, shaped by fluvial, eolian and glacial processes. The timeframe of these events is, however, poorly established. We describe efforts and challenges to adapt optically stimulated luminescence (OSL) dating for robotic in-situ dating of martian sediments. Mineral mixtures were devised as simulants of martian regolith. The single-aliquot regeneration (SAR) procedure was modified to enable the determination of the equivalent dose for polymineral samples. Low-temperature measurements and simulations indicate that known doses delivered at low temperatures can be effectively estimated as long as the stimulation temperature is greater than the highest temperature experienced during the initial irradiation. Bleaching experiments with a solar simulator suggest efficient zeroing of the OSL signal for solar-exposed sediments on Mars. Irradiations with proton and heavy-charged particles show a lower efficiency in luminescence production than that found for beta and gamma radiation.

© 2007 Elsevier Ltd. All rights reserved.

Keywords: Luminescence dating; OSL; Mars; Cosmic radiation

1. Introduction

When Mariner 4 transmitted the first close-range images of Mars in 1965, the pictures showed a frozen, barren and crater-pitted world. This disappointed many who had expected an environment that could sustain life. Later missions such as the Viking probes, the European Space Agency (ESA) Mars Express, and the NASA Mars Global Surveyor spacecraft revealed features that indicate Mars may once have been warmer and wetter. Although questions about the existence of life and water on the Red Planet can still not be answered conclusively, studies indicate that Mars might even today be a climatically active planet with obliquity changes modulating the climate (e.g.

Márquez et al., 2004). These changes in insolation have been determined to have a 51 ka cycle (Laskar et al., 2002).

Pictures taken by the High-Resolution Stereo Camera on-board the ESA Mars Express probe, as well as by the Mars Orbiter Camera (Mars Global Surveyor spacecraft, NASA), reveal intriguing landforms which appear to have been formed by large quantities of flowing water, eolian processes, and glacial processes. Deltas and lakes have been identified that likely formed during the Noachian (ending 3.8 or 3.5 Ga ago) or Hesperian (3.55–1.8 Ga) periods of Mars (e.g. Ori et al., 2000; Malin and Edgett, 2003; Mangold and Ansan, 2006). The origin of the extensive layering exposed in the Valles Marineris system is unknown, but might have been caused by fluvial sedimentary (e.g. Malin and Edgett, 2000) or volcanic events (e.g. McEwen et al., 1999; Williams et al., 2003). More recent features include gullies apparently formed by liquid water (e.g. Gilmore and Phillips, 2002) and aqueous floods and sediments (Baker, 2001; Burr and McEwen, 2002; Squyres

*Corresponding author. Radiation Dosimetry Laboratory, Venture I, Suite 201, 1110 S. Innovation Way Drive, Stillwater, OK 74074, USA. Tel.: +1 405 744 1013; fax: +1 405 744 1112.

E-mail address: regina.kalchgruber@okstate.edu (R. Kalchgruber).

and Knoll, 2005; Grotzinger et al., 2005). Ongoing climate changes are also reflected in the abrupt recession and rapid sublimation of the ice in the southern polar cap (Fishbaugh et al., 2000; Mustard et al., 2001; Malin et al., 2001; Thomas et al., 2005), as well as the apparent short accumulation history of the Polar Layered Deposits of the northern cap (Byrne and Murray, 2002; Laskar et al., 2002; Head et al., 2003; Milkovich and Head, 2005), or glaciers and rock glaciers (Baker, 2001; Cabrol et al., 2001; Cabrol and Grin 2002a, b; Mahaney et al., 2007). Detailed studies of images of the martian surface indicate that Mars has been, and continues to be, subject to feature-forming eolian activity (Greeley, 1992; Edgett and Malin, 2000; Albee, 2003; Armstrong and Leovy, 2005).

In advance of manned missions the exploration strategy for Mars is to carry out in-situ measurements via robotic instrumentation and to focus on: (i) evidence of life (extinct or extant); (ii) climatological history; and (iii) geological evolution (including the shaping of the present day surface features). Currently, the timing of geologic and climatic events is based upon relative crater densities and the assumption that the crater flux has been constant and similar to that of the Moon. This method however leads to uncertainties of the order of 1 Ma and more (Hartmann and Neukum, 2001; Hartmann, 2005) for younger ages. Several proposals have recently been advanced regarding possible in-situ instrumentation for dating of the geomorphological processes on the surface of Mars. A recent review discusses some of the potential and challenges of each of the proposed dating methods for this application (Doran et al., 2004). Optically stimulated luminescence (OSL) dating has been suggested as a technique that can be adapted for robotic in-situ dating of martian sediments that have been transported and deposited by wind or water over the last 10^4 – 10^5 years (Lepper and McKeever, 2000; Jain et al., 2006). In this context, efforts are being made to design miniature dating devices for in-situ luminescence dating of martian sediments (McKeever et al., 2003, 2006).

Use of a robotic luminescence dating instrument for Mars will require the development of new measurement techniques in order to deal with the multiple new challenges of the martian environment not usually found when using OSL to date terrestrial sediments. In luminescence dating the age is determined from the radiation dose, absorbed in the minerals since deposition, and the natural dose rate: $age = dose / dose\ rate$. Any method developed must therefore allow for the challenges in the determination of both, the dose and the dose rate.

A clear prerequisite to this development is the identification of the predominant minerals likely to be found in the martian regolith, and to examine the fundamental thermoluminescence (TL) and/or OSL properties of these materials (dose response, fading/stability, stimulation spectrum, etc.), in order to assess their suitability for luminescence dating. Previous OSL studies have focused on the general luminescence properties of the martian soil simulant JSC Mars-1 (Lepper and McKeever, 2000; Banerjee et al.,

2002b). Kalchgruber et al. (2006) used mineral mixtures, known as OSU Mars-1 and OSU Mars-2, as surrogates for the martian regolith.

Chemical separation of minerals will likely not be possible or limited on a robotic dating instrument and so it is projected that the procedure must be applicable to a mixture of minerals. As most luminescent materials on Mars are assumed to be some sort of feldspar, Blair et al. (2005) concentrated on modifying the single-aliquot regeneration (SAR) procedure so that it can be used effectively with feldspathic materials. Based on these studies, Kalchgruber et al. (2006) suggested a measurement procedure for the OSU Mars-1 and -2 martian regolith simulants. It is also necessary to consider that the ambient temperatures on the martian surface are significantly lower than on Earth, with large variations (from -140 to $+20$ °C). Thus, the influence of the temperature variation during the irradiation period on evaluated dose must be determined.

The entire premise of OSL dating is that the sediments to be dated have been exposed to sufficient amounts of light at the time of deposition to erase any previously accumulated signal. In terrestrial applications, this “zeroing” of the signal is accomplished within a few minutes of exposure to sunlight (Aitken, 1998), but the solar spectrum on Mars is different from that on Earth and may lead to different bleaching efficiencies. This requires a study of the efficiency of the martian solar spectrum at bleaching the TL/OSL under ambient conditions.

Another challenge is the radiation environment encountered at the surface and in the regolith of Mars. Background radiation from U, Th and K will not be the dominant radiation source in the upper (2–3 m) of the surface. Instead the radiation field will probably be dominated by high energy galactic cosmic rays (GCR) and solar energetic particles (SEP). Thus, to determine the rate at which the sediments have been irradiated requires studies of GCR and SEP radiation transport through the atmosphere and the martian regolith, and of the efficiency with which these energetic particles produce luminescence compared with the calibration radiation source on-board the robotic instrument.

In this publication we describe efforts and challenges to adapt OSL dating for robotic in-situ dating of martian sediments. Mineral mixtures were devised as simulants of martian regolith and the SAR procedure was altered to determine the equivalent dose for these polymineral samples. Experiments and computer simulations to investigate the temperature dependence of the luminescence emission are presented. The bleaching and fading behaviors of the minerals are discussed. We describe experiments with proton and heavy-charged-particle irradiations to determine the response of the regolith simulants to the cosmic radiation at the surface of Mars. The luminescence efficiency of the particles is compared to beta radiation and the doses measured at various depths in the regolith simulant are also discussed.

2. General principles of luminescence dating

OSL dating works on the principle that ionizing radiation from U, Th, K, as well as from cosmic rays ionizes atoms within silicate mineral grains like quartz and feldspar. A portion of these freed electrons become trapped at crystal defects within the mineral, some of which are light sensitive. The number of trapped electrons increases over geologic time and is a direct measure for the energy deposited in the mineral by ionizing radiation. Exposure to heat or sunlight resets or “zeroes” the luminescence clock by releasing (“bleaching”) the electrons from the traps. When some of the electrons recombine with charges of the opposite sign, the light emitted during this process by the minerals themselves is called thermally stimulated luminescence (TL) or OSL. The luminescence signal is a direct measure for the number of trapped charges, and is proportional to the time elapsed since the mineral grains were last exposed to daylight (i.e., the time since burial). If the mineral grains are shielded from further sunlight by burial, trapped electrons begin to re-accumulate.

In the laboratory feldspar or quartz separates are prepared from the sediments. The measurements simulate the natural luminescence process. The sample is stimulated with light of one wavelength (e.g. blue or infrared), and the OSL emitted from the sediment is monitored at another wavelength (e.g. UV). The intensity of this “natural” luminescence signal is proportional to the energy from ionizing radiation absorbed since burial. The amount of absorbed energy, the “equivalent dose” (D_e , unit: Gray; $1 \text{ Gy} = 1 \text{ J/kg}$), is determined by comparing the natural luminescence signal with the signals obtained after known radiation exposures administered in the laboratory. The rate of natural irradiation, the “dose rate” (in Gy/yr), can be determined from the concentration of radioactive nuclides (U, Th, K) in the sediment. Assuming a constant dose rate, the burial age of the sample is then derived from $age = equivalent\ dose / dose\ rate$.

Several methods have been used to obtain the equivalent dose from the measured luminescence signal. The most revolutionary development of the last decade was the development of the so-called single-aliquot regenerative-dose method (SAR; Murray and Wintle, 2000; Wintle and Murray, 2006). Measurements are carried out with subsamples (aliquots) of only 1–2 mg (~100–1000 grains). A dose value can be obtained for each single aliquot and the total equivalent dose is calculated as the average of all measured aliquots of a sample.

The range of OSL dating is from recent decades (e.g. Madsen et al., 2005) to 700,000 years ago (Banerjee et al., 2003; Olley et al., 2004; Watanuki et al., 2005). The lower age limit is determined by the lower detection limit of the OSL signal. For high doses the signal ceases to increase with increasing dose, which means that an upper measurable dose exists. The upper age limit therefore depends on the saturation region of the dose response as well as the

natural dose rate. Higher ages can be obtained for lower dose rates. The uncertainty is usually about 10%. Detailed discussions of luminescence dating methods including equivalent dose and dose rate determination can be found in publications by Aitken (1985, 1998) and by Wintle (1997).

3. Experimental details

All conventional OSL measurements at room temperature or above were made using a Risø TL/OSL-DA-15 reader (Risø National Laboratory; Bøtter-Jensen et al., 2000) with a bialkali PM tube (Thorn EMI 9635QB) and Hoya U-340 filters (290–370 nm). The built-in $^{90}\text{Sr}/^{90}\text{Y}$ beta source gives a dose rate of ~100 mGy/s for 90–250 μm quartz. Optical stimulation was carried out with blue LEDs ($470 \pm 30 \text{ nm}$), delivering 31 mW/cm^2 to the sample; IR stimulation was from an IR LED array at $875 \pm 80 \text{ nm}$ with 100 mW/cm^2 delivered to the sample. The heating rate used was $5 \text{ }^\circ\text{C/s}$. All samples were bleached prior to measurement by stimulating with IR and blue diodes, each for 1000 s at room temperature.

TL spectra were measured using a Jobin–Yvon Fluorolog spectrofluorometer with Czerny–Turner spectrometer and a photomultiplier tube for luminescence detection.

The low-temperature TL and OSL measurements were made using the low-temperature TL/OSL system described in Blair et al. (2006b), with a liquid nitrogen cryostat allowing temperatures from -150 to $200 \text{ }^\circ\text{C}$ to be obtained. Due to the low-temperatures reached during experiments, the cryostat was maintained at a vacuum level of approximately $5 \times 10^{-4} \text{ Torr}$ by a turbomolecular pump. Nitrogen flow and 50 W pencil heaters from Watlow were controlled by an Omega CN3251 temperature/process controller and custom control box. Luminescence detection was accomplished by an EMI 9635QB PMT using a Stanford Research SR400 photon counter, and a filter pack containing Hoya U-340 filters. Irradiation was carried out using a 40 kVp (tube peak potential) Moxtek miniature X-ray system that delivered 0.045 Gy/s (calibrated against one of the previously described Risø systems). Optical stimulation was done using a 100 mW diode pump solid-state green laser (532 nm) from Extreme Lasers Inc. (USA) operating in continuous-wave mode and delivering approximately 10 mW/cm^2 at the sample position.

4. Progress toward equivalent dose determination

4.1. Mineral identification

An in-situ OSL dating instrument for martian surface sediments will likely not allow chemical treatment and mineral separation of the regolith samples. The measurement of the equivalent dose therefore requires a procedure that is suitable for polymineral samples, with mineral mixtures that are not commonly found on Earth. Sample return missions to and from Mars are planned only beyond

2018. Martian meteorites are the only martian materials currently available and their basic luminescence properties have been studied by Banerjee et al. (2002a) and Blair et al. (2003). Most martian meteorites, however, do not match well with the spectral characteristics of the martian surface and therefore may not be representative of martian regolith (Bandfield, 2002).

Several materials have been adopted to simulate the regolith on Mars. The selection criteria have been based on the intended applications. “JSC Mars-1”, from the Pu’u Nene volcano on Mauna Kea, Hawaii, was selected by Allen et al. (1998) as a regolith simulant based upon reflectance spectra. This material was chosen because of its similarity to the martian regolith in physical and chemical composition. It consists of magnetic and non-magnetic fractions, both of which are made up of feldspar, magnetite, pyroxene, olivine, and volcanic glass. Previous OSL studies have focused on the general luminescence properties of “JSC Mars-1” (Lepper and McKeever, 2000; Banerjee et al., 2002b).

More recent data from the thermal emission spectrometer (TES) aboard Mars Global Surveyor (MGS) has suggested slightly different mixtures of minerals for analogs of martian regolith. Spectra from these instruments distinguish two different types of regolith on Mars, namely Type I (basaltic mineralogy) and Type II (andesitic mineralogy). Both types of regolith, according to the TES

results, are composed of plagioclase feldspars, pyroxenes (primarily augite and diopside), and hematite, and the Type II material contains an abundance of obsidian or volcanic glass (Bandfield et al., 2000; Bandfield, 2002). Plagioclase feldspars are found to have a calcium content of 30–70% (Milam et al., 2004). Based on these data we devised two mineral mixtures as surrogates for martian sediments (Kalchgruber et al., 2006). The compositions of the mixtures OSU Mars-1 and -2 are given in Table 1. OSU Mars-1 and -2 are the two mineral mixtures used through this paper as surrogates for polymineralic martian sediments.

The TL-emission spectrum of OSU Mars-2 (Fig. 1; corrected for the wavelength response of the detection system) reveals a dominant red emission and weaker emissions in the blue and UV wavelength band. Kalchgruber et al. (2006) found that a major part of the signal emitted by the mineral mixtures originates from the feldspars labradorite and andesine, with minor contributions from diopside. Due to the difficult separation of stimulation light and emission in the red wavelength band we focused in our experiments on the UV-emission.

4.2. SAR procedure for polymineral mixtures and dose-recovery experiments

Sediment samples for terrestrial applications usually undergo an elaborate preparation procedure in the laboratory including wet-chemical treatment and density separation. Basic treatments such as sieving and separation of magnetic minerals are probably possible for in-situ measurements on Mars. It is, however, desirable to avoid the more complex use of chemicals. Quartz has not been found in abundance on Mars, and most regions seem dominated by feldspathic minerals. But, as described above, minerals like pyroxenes will contribute to the luminescence signal as well. A measurement procedure must therefore be suitable for polymineral mixtures.

Table 1
Composition of the martian regolith simulants OSU Mars-1 and -2

	OSU Mars-1 (%)	OSU Mars-2 (%)
Andesine	22	15
Labradorite	22	15
Bytownite	22	15
Augite	15	5
Diopside	15	5
Hematite	5	5
Obsidian		40

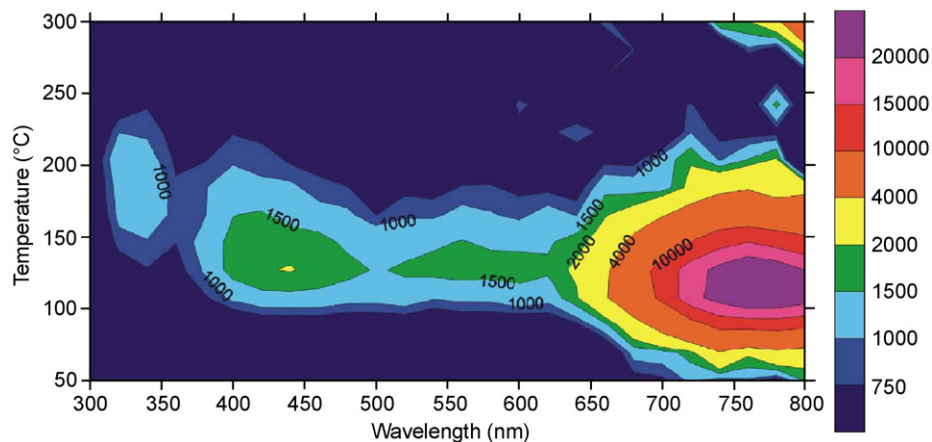


Fig. 1. TL emission spectrum of OSU Mars-2, corrected for the response of the detection system, after irradiation with 100 Gy. The numbers in the figure and the color scale indicate the measured counts.

Table 2

Measurement procedure for martian regolith simulants suggested by Kalchgruber et al. (2006)

1. Regeneration radiation dose (D_i).
2. Preheat at 210 °C for 10 s.
3. Measure IRSL at 60 °C for 300 s (R_iI).
4. Measure OSL at 150 °C for 300 s (R_iO).
5. Fixed test radiation dose (TD_i).
6. Cutheat to 210 °C.
7. Measure IRSL at 60 °C for 300 s (T_iI).
8. Measure OSL at 150 °C for 300 s (T_iO).
9. Repeat steps 1–6 for a range of regeneration doses.
10. Find sensitivity-corrected IRSL, L_iI , and OSL, L_iO ($L_i = R_i/T_i$).

For dose recovery:

- Cycle 1: Known dose D_1 for dose recovery
 Cycles 2–5: Dose response with $D_2, D_3 < D_1$ and $D_4, D_5 > D_1$
 Cycles 6 and 7: Repeat doses with $D_6 = D_1$ and $D_7 = D_2$

The SAR procedure (Murray and Wintle, 2000) has proven to be an effective method of equivalent dose, D_e , estimation for coarse-grain quartz. The major advantages of the SAR include the ability to produce an age from one aliquot and to correct for any sensitivity changes during the measurement procedure. With slight modifications, the SAR procedure has also been adapted for polymineral fine-grain materials (Banerjee et al., 2001; Roberts and Wintle, 2003) and quartz samples with significant feldspar contamination (Wallinga et al., 2002) by using a combined IR and blue (“post-IR blue”) stimulation sequence to isolate a quartz-dominated signal. More recent work has shown that sensitivity changes in feldspars can be corrected by the SAR procedure if the same preheat treatment is used after test and regeneration doses (Auclair et al., 2003; Blair et al., 2005). In addition, using a post-IR blue stimulation sequence potentially allows the isolation of feldspar- and quartz-dominated signals as well as extending the accessible age range for feldspars (Blair et al., 2006a).

Based on these results, Kalchgruber et al. (2006) carried out experiments to find the most suitable measurement procedure for the mineral mixtures used as martian regolith simulants. They suggest using a post-IR blue SAR procedure, with a 210 °C preheat with no hold after the test dose and a 210 °C preheat for 10 s after the regeneration dose, with IR stimulation at 60 °C, and OSL readout at 150 °C. The $^{90}\text{Sr}/^{90}\text{Y}$ beta test dose was 15–20% of the initially administered dose. The measured OSL signals are integrated over the first 10 s, while the background for subtraction is obtained from the last 5 s of stimulation. A summary of the suggested procedure is listed in Table 2.

Kalchgruber et al. (2006) extensively describe the testing of the procedure for dose-recovery experiments. They found that the dose response could be fitted linearly using a local slope approximation to determine doses as high as 1600 Gy. Although a post-IR blue procedure is more power-consuming than an IR- or OSL-only procedure, it

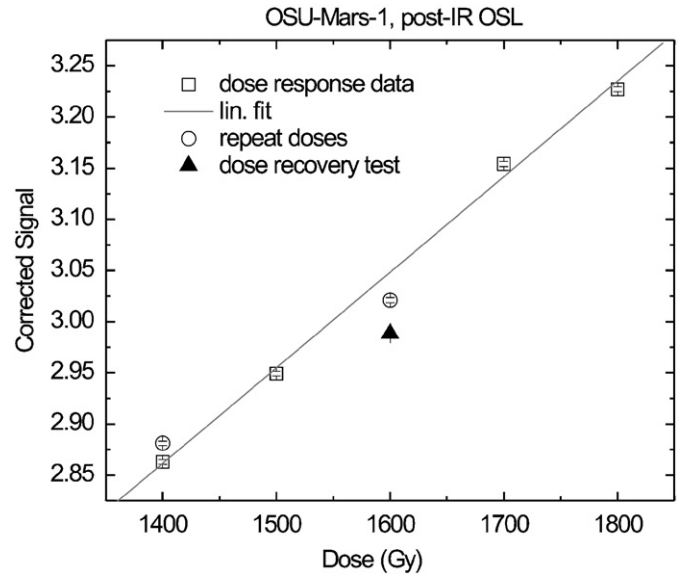


Fig. 2. Sensitivity-corrected local dose–response curves for the post-IR OSL signal of OSU Mars-1. The symbols are described in the legend. The line indicates the linear fit.

yielded better results for high doses. The accuracy for a 1600 Gy laboratory dose was 6.1% using the IR stimulated luminescence (IRSL) signal and 4.0% for the post-IR OSL (see Fig. 2). The calculated uncertainties for the doses, resulting from the statistical uncertainty of the signal and the fitting parameters were 10% and 5.5%, respectively, i.e., slightly larger. Additionally the procedure has the advantage that two independent dose values are measured. With the possibility of using the local slope for dose recovery it is not necessary to build up a whole dose response starting from zero.

Jain et al. (2006) determined visually the apparent saturation levels of various minerals expected on Mars. The values ranged from 2.5 kGy for *ortho*-pyroxenes to more than 12 kGy for basalt. Banerjee et al. (2002b) fitted the dose response with a single saturating exponential and determined a theoretical maximum estimable dose. We used the procedure listed in Table 2 to measure a sensitivity-corrected dose response (test dose 1 Gy). The IRSL and post-IR OSL dose responses for both OSU Mars-1 and -2 are plotted in Fig. 3. We found a good agreement between data and fit using a double saturating exponential of the form

$$L = A_1(1 - \exp(-D/D_{c1})) + A_2(1 - \exp(-D/D_{c2})),$$

where L is the sensitivity-corrected luminescence, $A_1 + A_2$ is the asymptotic value of the sensitivity-corrected luminescence, D is the dose, and D_{c1} and D_{c2} are the characteristic doses. If the luminescence signal consisted of only one component, A would represent the maximum or asymptotic value of the signal. The signal reaches 95% of the maximum possible value for $D = 3D_c$. We used this relationship, for comparison purposes only, to determine a theoretical maximum estimable dose from D_{c2} (with $D_{c2} > D_{c1}$).

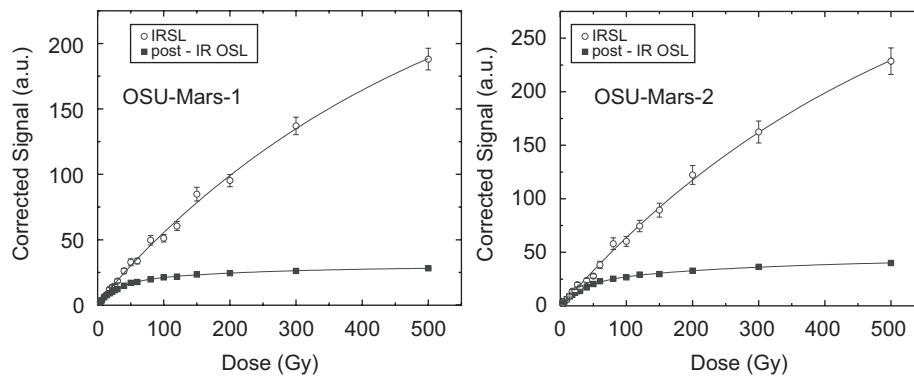


Fig. 3. Sensitivity-corrected dose–response curves for OSU Mars-1 (left) and OSU Mars-2 (right). The figures show data for infrared-stimulated OSL as part of a post-IR blue stimulation sequence and the post-IR OSL. The lines indicate the fits with double saturating exponentials.

In both cases the OSL signal saturates at lower doses than the IRSL signal. The theoretical maximum estimable doses using the IRSL signal are 1500 Gy for OSU Mars-1 and 1600 Gy for OSU Mars-2. Using the post-IR blue signals the values were 570 and 870 Gy. These values describe theoretical maxima for comparison purposes only and do not necessarily represent actual measurement limits. Kalchgruber et al. (2006) showed that doses as high as 1600 Gy can be recovered with the post-IR blue signal. They also found that small test doses do not correct sufficiently for the sensitivity changes. A 100 Gy dose could be recovered with 3.2% accuracy using a 20 Gy test dose. When a 1 Gy test dose was used, the accuracy for the recovered dose was 14% only. The accuracies worsened considerably for higher doses with the 1 Gy test dose, but remained around 5%, if the test dose was 15–20% of the administered dose. In the present experiments a 1 Gy test dose was used for all measurements, including doses as high as 500 Gy, and thus it can be presumed that sensitivity changes were not fully corrected. The maximum estimable doses are, therefore, expected to be higher than these semi-empirically determined values.

4.3. Low-temperature measurements

In terrestrial applications, most minerals dated by OSL are assumed to have been near room temperature (20 °C) for the entirety of their storage period. However, on Mars the average ambient temperature is much lower (−63 °C) with a large annual variation (−133 to 27 °C) (Kieffer et al., 1992). A lower storage temperature can have profound implications for the procedures used to recover the natural radiation dose (e.g., the preheat temperature and duration, the stimulation/measurement temperature) and the design of the robotic instrument (e.g., temperature control equipment). In order to test the effect of low ambient temperature on the OSL process we used the low-temperature TL/OSL system described in Blair et al. (2006b).

The low-temperature TL/OSL system was used to measure radioluminescence (RL, luminescence signal emitted during irradiation), TL, and OSL of various materials (the martian soil simulants OSU Mars-1 and OSU Mars-2 being of most interest in this paper) that were irradiated and stimulated at varying temperatures between −125 and 200 °C. The minerals showed an increase in RL or luminescence efficiency with decreasing irradiation temperature, and the TL experiments showed that both OSU Mars-1 and OSU Mars-2 have optically active low-temperature TL traps. By varying the measurement conditions, it was also found that the OSL of the mineral mixtures depended upon both the irradiation and stimulation temperature. More important, however, are the results of the dose-recovery experiments conducted with the low-temperature TL/OSL system.

For the dose-recovery experiments, a known X-ray dose was delivered to the samples at −100 °C, and then the dose was estimated using a standard SAR dose estimation procedure while varying the irradiation and stimulation temperatures. The results of these experiments are summarized in Table 3. It was found that known doses delivered at low temperatures could be effectively estimated as long as the stimulation temperature was greater than or equal to the highest temperature experienced by the mineral during the initial irradiation. However, the results of numerical modeling of the low-temperature OSL process places even more stringent constraints on the dose-recovery procedure, as described below.

Two models of a generic luminescence system were used to numerically simulate the OSL process and thereby determine the effect of low ambient temperature on the luminescence process. Both models consisted of an optically active main dosimetric trap (TL peak near 300 °C, Level 1), a trap with a TL peak around 100 °C that is not optically active to simulate moderately shallow traps that act as competitors for charge (Level 2), a low-temperature, optically active trap with a TL peak near −50 °C (Level 3), a thermally disconnected deep trap

Table 3
Dose recovery experiments conducted in the low-temperature OSL system

Exp. no.	$T_{\text{irr,k}}$ (°C)	$T_{\text{irr,r}}$ (°C)	T_{OSL} (°C)	Dose ratio OSU Mars-1	Dose ratio OSU Mars-2
1	25	25	25	1.01 ± 0.25	1.02 ± 0.14
2	–100	–100	–100	1.07 ± 0.77	0.98 ± 0.11
3	–100	25	25	1.01 ± 0.04	0.94 ± 0.32
4	25	–100	–100	0.33 ± 0.64	0.26 ± 0.01
5	–100 ^a	–100	–100	0.60 ± 0.09	0.39 ± 0.15
	–50				
	25				
6	–100 ^a	25	25	0.95 ± 0.52	1.04 ± 0.28
	–50				
	25				

The temperature of the irradiation ($T_{\text{irr,k}}$) to known dose, the regeneration (and test) dose irradiation temperatures ($T_{\text{irr,r}}$), and the OSL measurement temperature (T_{OSL}) are given along with the dose recovered ratio (the dose ratio = recovered dose/administered dose) for OSU Mars-1 and -2. Note that in experiments 5 and 6 the known dose was delivered in stages at three different temperatures to simulate the diurnal temperature variation on Mars.

^a1.7 Gy delivered at each temperature.

Table 4
Parameters for the 4 traps and 1 recombination center used in the numerical simulations of low-temperature traps and the OSL process (see text for the equations used)

Level	N (cm ^{–3})	E (eV)	s (s ^{–1})	A (cm ³ /s)	A_m (cm ³ /s)
1*	10^{11}	0.6	5×10^{12}	^a 10^{-9} ^b 10^{-10}	–
2	^a 10^{11} ^b 10^9	0.9	5×10^{12}	^a 10^{-9} ^b 10^{-10}	–
3*	10^{11}	1.7	10^{14}	10^{-10}	–
4	^a 10^{11} ^b 5×10^{11}	–	–	10^{-10}	–
5	^a 1.1×10^{12} ^b 5×10^{12}	–	–	4×10^{-10}	2×10^{-9}

^aDenotes the parameter for Model A.

^bDenotes the parameter for Model B.

*Optically active.

Other parameters:

$f = 1 \times 10^8 \text{ cm}^{-3} \text{ s}^{-1}$ (irradiation rate $\sim 1 \text{ Gy/s}$).

$f_2 = 1 \times 10^{-2} \text{ s}^{-1}$ (optical excitation rate).

$\beta = \pm 5 \text{ °C/s}$ (heating rate).

(Level 4), and one thermally disconnected recombination center (Level 5). The two models differ in the concentration of the 100 °C trap; the 100 °C trap dominates the luminescence process in one model (Model A) and is relatively unimportant in the other model (Model B). These models are merely simple generic models and do not necessarily represent the regolith simulants. They are meant to act as a guide to how the experiments need to be performed and to have some understanding of the qualitative features of the behavior of these OSL systems. The parameters for these two models are given in Table 4, and the simulations were carried out using the following

Table 5
Results of dose recovery and dose estimation simulations with both energy level models (A and B)

Nat. Irr. T (°C)	Irr. T (°C)	OSL T (°C)	Dose ratio	
			Model A	Model B
–100	–100	–100	0.08	0.55
–100	–100	25	0.19	1.02
–100	25	25	0.17	1.02
Variable	25	25		1.00
Variable	–100	20		1.00
Variable	–100	–100		0.55

In these simulations, the laboratory or natural dose was delivered at either –100 °C or at an average of –60 °C with a yearly variation of 80 °C. Irradiation and stimulation was carried out at the specified temperature.

rate equations:

$$\frac{dn_c}{dt} = f + \sum_i n_i f_2 + \sum_i n_i s_i \exp\left(\frac{-E_i}{k_B T}\right) - n_c \times \sum_i (N_i - n_i) A_i - n_c m A_m,$$

$$\frac{dn_i}{dt} = -n_i f_2 - n_i s_i \exp\left(\frac{E_i}{k_B T}\right) + n_c (N_i - n_i) A_i,$$

$$\frac{dm}{dt} = n_v (M - m) A - n_c m A_m,$$

$$\frac{dn_v}{dt} = f - n_v (M - m) A,$$

$$T = T_0 + \beta t.$$

Several simulations confirmed that the two models could reproduce most of the TL and OSL characteristics. We simulated irradiation at a natural dose rate (2 mGy/yr) that was delivered at –100 °C, and an average of –60 °C with a yearly variation of 80 °C (the temperature variation simulation was only carried out with Model B), and then tried to model the recovery of that dose in the same way as we had done in the experiments. The results are summarized in Table 5. These simulations revealed that if the luminescence process is dominated by a trap similar to the 100 °C trap the natural dose cannot be accurately estimated. In addition, it was found that the stimulation temperature must be significantly higher than the highest irradiation temperature in nature, i.e. the stimulation temperature should be at least 80–100 °C on Mars where the highest temperature is expected to be around 20 °C. This requirement is due to the fact that charge does not accumulate in low-temperature traps (i.e., the –50 °C trap) during irradiation at natural dose rates as the traps are not stable over long time scales. However, low-temperature traps do retain charge during irradiation at laboratory dose rates since the irradiation is almost instantaneous.

4.4. Solar bleaching

As OSL dating seeks to determine the last time that sediments were exposed to light, the effective removal of

trapped charge at deposition is critical to the process. The solar spectrum on Earth is well known, and solar resetting under terrestrial conditions has been investigated extensively. The “zeroing” of the signal is accomplished within a few minutes of exposure to sunlight (Aitken, 1998). The solar spectrum on Mars, however, is different from that on Earth and may lead to different bleaching efficiencies, as discussed by McKeever et al. (2006).

No measured data exist for the spectral irradiance at the surface of Mars. Many radiative transfer calculations for the atmosphere of Mars have focused on the UV range of the solar spectrum, due to its potential influence on life forms and atmospheric photochemical reactions (e.g. Patel et al., 2002). Extensive simulations, triggered by the data from TES, have also been carried out in the thermal IR region (e.g. Wolff and Clancy, 2003). However, almost no data exist for the visible spectral range.

The wavelength range between 200 and 900 nm is particularly important for the solar resetting of sediments. Therefore, we carried out radiative transfer calculations for the atmosphere of Mars using the libRadtran software package of Mayer and Kylling, (2005), which is freely available under the GNU General Public License (<http://www.libradtran.org>). The calculation is based on a vertical atmospheric profile and accounts for absorption by CO₂, O₂, O₃, and H₂O, as well as Rayleigh scattering. Lambertian surface albedo and extinction by dust particles were also included. Minor changes were necessary to adapt the package for martian conditions. A more detailed description of the simulations is given by Deo et al. (2005).

Fig. 4 shows the results of the solar spectrum calculation for Mars. A comparison of the total spectral irradiances for

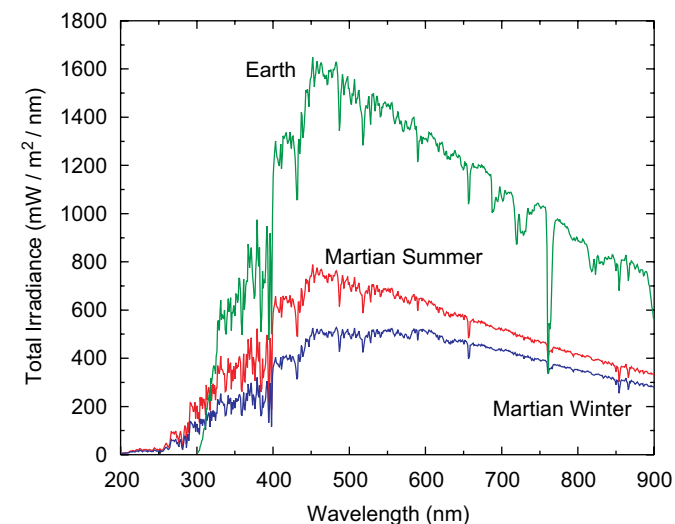


Fig. 4. Solar spectra for Earth and Mars. Both spectra were calculated for 20° latitude and noon conditions. For the day in northern summer the areocentric longitude was 143°, solar zenith angle 5°, dust optical thickness $\tau_{\text{dust}} = 0.1$, 0.1 DU ozone and 0.02 mm precipitable water. For the northern winter the areocentric longitude was 250°, solar zenith angle 43°, $\tau_{\text{dust}} = 1$, 0.2 DU ozone and 0.01 mm precipitable water. (Note: 1 DU ozone = $2.69 \cdot 10^{16}$ part/cm²; an optical thickness of 0.1 reduces the intensity of light by $e^{-0.1}$.) (Fig. 1 from McKeever et al., 2006).

a clear day on Earth (solar zenith angle 20°) and typical summer and winter days on Mars are shown. The integrated (200–900 nm) total irradiance at the surface of Mars is similar for both seasons. The irradiance in the northern summer amounts to 49% of the value for Earth. Due to the higher dust load and the increased solar zenith angle in winter, the irradiance is only 37% of the Earth value. Whereas practically no radiation below 300 nm reaches the surface of Earth, sediments on Mars are exposed to UV radiation starting from 200 nm. The results indicate that 9% of radiation on Earth comes from the UV range whereas the values for the martian summer and winter are 12% and 10%, respectively. Although the relative UV-irradiance are comparable for both planets, it has to be taken into account that, unlike Earth, about 15% of the UV-irradiance on Mars is caused by radiation with wavelengths smaller than 300 nm.

The bleaching efficiency increases for shorter visible wavelengths (see e.g. Aitken, 1998). Exposure to UV wavelengths, however, has been found to build up latent IRSL and OSL in feldspars (Bailiff and Poolton, 1991; Poolton et al., 2006), which was attributed to phototransfer. The higher short-wave UV component in the solar spectrum, as well as the smaller total irradiance may therefore have profound consequences for OSL dating. We have simulated the martian spectrum with a 150 W Oriel Solar Simulator with a UV-enhanced xenon lamp and tested the bleaching characteristics of the martian regolith simulants. An air-mass-0 filter (Oriel) corrects the output spectrum of the lamp to better match the emission spectrum of the sun at the top of the atmosphere, without absorption or attenuation by components in the Earth’s atmosphere. The resulting spectrum was considered a sufficiently close match of the spectral irradiance at the surface of Mars. The total power of the solar simulator in the UV and visible regions was adjusted to 31 mW/cm², the expected power at the surface of Mars. The samples were first fully bleached by reading either the OSL or the IRSL signal at room temperature for 1000 s, and afterwards given a dose of 15 Gy. On each occasion 4 sample disks were exposed to the solar simulator at room temperature, and the residual OSL signal was measured. The preheat temperature was 210 °C for 10 s. IR stimulation and OSL stimulation were carried out for 300 s at 60 and 150 °C, respectively. The signal from another 15 Gy dose was used for sensitivity correction (see also McKeever et al., 2006). The data for mixture OSU Mars-1 show that the IRSL signal bleaches faster than the blue-stimulated OSL signal. After 10 min of exposure to the solar simulator only 5% of the original IRSL signal (10% for blue-stimulated OSL) is left and after 200 min the sample is fully bleached (see Fig. 5).

4.5. Fading

A remaining significant issue for the estimation of the equivalent dose is anomalous fading. The martian regolith

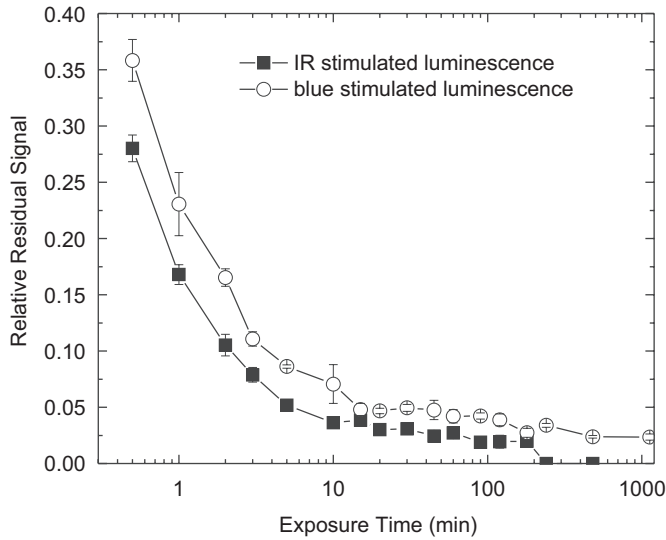


Fig. 5. Effects of martian solar bleaching on the IRSL and OSL signals from sample OSU Mars-1. (Fig. 2 from McKeever et al., 2006).

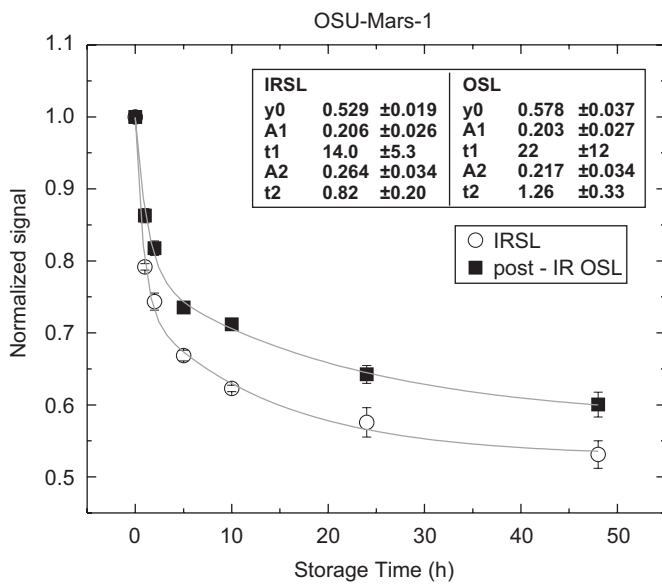


Fig. 6. Fading measurement of OSU Mars-1. The signal was normalized to the signal measured directly after irradiation. Error bars are standard errors determined from three aliquots. The lines indicate fits with double exponential decay curves, the fitting parameters are listed.

has been shown to consist of feldspars to a high degree. Feldspars have been found to show a loss of signal during storage (e.g. Huntley and Lamothe, 2001), known as athermal or anomalous fading. Fig. 6 shows initial fading tests for OSU Mars-1. We used the sequence listed in Table 2. As suggested by Auclair et al. (2003), the samples were irradiated and preheated (at 210 °C, for 10 s) before the storage period. The sensitivity-corrected signal was normalized to the corrected signal measured directly after irradiation. The experiments indicate that the fading is initially rapid, but stabilizes after a few days. The signals were fitted with double exponential decay curves of the

form

$$L = y_0 + A_1 \exp(-t/t_1) + A_2 \exp(-t/t_2),$$

where L is the sensitivity-corrected luminescence, A_1 and A_2 are the amplitudes, t is the storage time, t_1 and t_2 are the characteristic decay constants, and y_0 is the offset or asymptotic value. The y_0 values for IRSL and post-IR OSL are 0.53 and 0.58, respectively, suggesting that 53% of the IRSL and 58% of the OSL signal are stable. The measured remaining signals after 48 h are 0.53 and 0.60, indicating that the unstable signals have already completely decayed after 2 days. We subtracted the stable signal components from the total measured signal and determined the fading rate (g -value) as described by Huntley and Lamothe (2001) for the remaining signal components. The resulting fading rates were 64% per decade for the IRSL signal and 60% per decade for the OSL signal. This issue will require further and detailed examination. If the observation is confirmed in later experiments one may have a situation where the unstable component has already faded in any martian sediment sample that is extracted for OSL measurement. It is intended to further characterize the fading properties of the regolith simulants and to determine an adjustment of the measurement procedure to correct for signal instability. The most likely and least energy consuming means is to allow time for fading after each calibration irradiation. Another possibility that we plan to investigate is the use of the strong red OSL emission signal (see Fig. 1), since Fattahi and Stokes (2003) found the red emission of feldspars to be less prone to fading.

5. Progress toward dose rate determination

5.1. The radiation environment on Mars and the physical context

A challenge equal to that of assessing the equivalent dose is determining the natural dose rate at the surface and in the regolith of Mars is. In terrestrial applications the total dose rate, \dot{D} , is the sum of the single contributions by alpha, beta, gamma, and cosmic radiation:

$$\dot{D} = a\dot{D}_\alpha + \dot{D}_\beta + \dot{D}_\gamma + \dot{D}_{\text{cosmic}}.$$

Alpha radiation has a smaller efficiency in luminescence production than beta or gamma radiation, which is corrected by including a correction factor a in the equation. This so-called a -value is determined for each sample separately and is often found to be close to 0.1 (see e.g. Aitken, 1985). The contribution of cosmic radiation to the total dose rate is usually in the order of only 5%. The cosmic dose rate is simply calculated as described by Barbouti and Rastin (1983) and Prescott and Stephan (1982), using the geographic coordinates and the burial depth of the sample.

Unlike Earth, background radiation from U, Th and K, as derived from meteorites (e.g. Shubert et al., 1992), is not

the dominant radiation source in the upper 2–3 m of the martian surface. The main source for the dose rate on Mars is from galactic cosmic rays (GCR) and solar energetic particles (SEP). The GCR spectrum consists of approximately 85% protons, 12% alpha particles, 1% heavier nuclei, and about 2% electrons and positrons (Benton and Benton, 2001). The energies range from several tens up to 10^{12} MeV with a broad peak between 0.1 and 1 GeV. Solar energetic particles include electrons, protons and heavier ions, and ~ 50 events can be expected in the 11-year solar cycle (for a detailed description, see e.g. Benton and Benton, 2001).

For a constant administered dose, the intensity of the luminescence signal depends on the type and energy of ionizing radiation. With increasing ionization density, described by the linear energy transfer (LET) of a particle, more charge carriers are released in the same crystal volume. The limited number of crystal defects leads to an increasing number of instantaneous recombinations. The result is a smaller percentage of trapped charges and a smaller luminescence signal/per unit dose for heavy-charged particles compared to beta radiation or high energy photons. The dominating beta and gamma radiation in the terrestrial environment have similar LET. The greater GCR contribution in the case of Mars, however, makes it necessary to allow for the varying LETs of the particles. Since the equivalent dose will be determined in relation to an X-ray or beta source in a robotic instrument, the relative efficiency of the GCR in producing OSL compared with the on-board radiation source needs to be determined, in analogy to the a -value described above.

Dose rates expected on the martian surface (dependent upon altitude) are typically of the order ~ 80 – 120 mGy/yr (Saganti et al., 2004). Furthermore, the composition of the cosmic radiation field will change with increasing depth in the regolith due to absorption and scattering. At a depth of 25 g/cm² the dose rate is estimated to be 200 mGy/yr, while at 700 g/cm² the dose rate is expected to be reduced to approximately 0.5 mGy/yr (Pavlov et al., 2002; see also McKeever et al., 2003). Thus, to determine the rate at which the sediments have been irradiated requires studies of GCR radiation transport through the atmosphere and the martian regolith, and measurements of the efficiency with which these radiation types produce OSL compared with the calibration radiation source on-board the luminescence dating instrument.

5.2. Description of radiation experiments

For the determination of the natural dose rate the following questions need to be answered: (1) what is the efficiency (compared to X-, beta or gamma irradiation) of OSL production for the particles and energies encountered in GCR and SEP radiation at the surface of Mars? (2) How does this efficiency change with increasing depth in regolith?

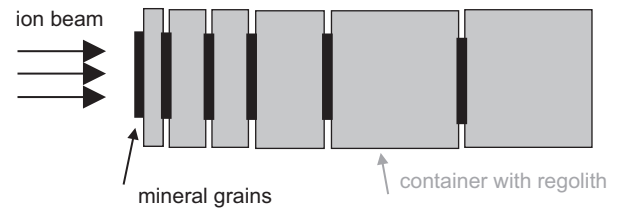


Fig. 7. Simplified diagram of the experimental setup used at HIMAC and NSRL.

To this end we carried out accelerator-based experiments with simulated cosmic rays at the Heavy Ion Medical Accelerator (HIMAC) in Chiba, Japan, and the NASA Space Radiation Laboratory (NSRL) at Brookhaven National Laboratory. During the irradiations, small containers with OSU Mars-1, -2, and sedimentary quartz were sandwiched between columns of martian regolith simulant of various thicknesses, simulating a variety of burial depths in the martian regolith (Fig. 7).

Sample containers were 0.3 mL plastic vials, with an outer diameter of 0.7 cm and a 1 cm height. Even though the abundance of quartz on Mars is expected to be low, we added quartz to our experiment due to the similar luminescence and radiation absorption properties to the abundant feldspars, and the lack of anomalous fading of its OSL signal. The martian regolith-simulant in the columns consisted of 45.4% SiO₂, 24.3% Al₂O₃, 16.3% Fe₂O₃, 6.5% CaO, 3.5% MgO and 4.0% TiO₂, and had a composition similar to JSC Mars-1 described by Allen et al. (1998).

The minerals were irradiated with known doses of 1 GeV protons, 150 MeV/u He, 500 MeV/u Fe and 1 GeV/u Fe (1 MeV/u = 1 MeV per each nucleon; a 150 MeV/u helium ion has a total energy of 150 MeV/u * 4 nucleons, i.e. 600 MeV). The size of the spatially uniform ion-beam was 10 cm × 10 cm. The ion-doses at zero regolith-depth were 5 Gy for protons and 10 Gy for all other ions (doses measured in water). The doses in water were converted to dose in mineral at zero regolith-depth, D_{ion} , using the respective densities and LET values for each mineral.

Luminescence measurements with OSU Mars-1 and -2 were based on the IR-blue procedure in Table 2, without the test-dose corrections. The quartz samples were pre-heated for 10 s at 240 °C and stimulated with blue diodes only at 125 °C for 300 s. Measurements were carried out with the Risø TL/OSL reader described above. The quoted beta doses, D_{β} , are doses to quartz. The following sequence of measurements was used:

1. Measure IRSL and/or OSL signals resulting from the ion irradiation, OSL_{ion} .
2. Give beta dose (5 or 10 Gy).
3. Measure IRSL and/or OSL signals resulting from the beta irradiation, OSL_{β} .
4. Give beta dose, D_{β} .
5. Wait for same period as that elapsed between ion irradiation and step 1, OSL_{β} .

6. Measure IRSL and/or OSL signals resulting from the beta irradiation after fading.
7. Give beta dose (5 or 10 Gy).
8. Measure IRSL and/or OSL signals resulting from the beta irradiation, OSL_2 .

After the ion irradiations at the accelerators, the samples had to be shipped to OSU. Several days to weeks elapsed before the measurements could be started. To allow for anomalous fading of the signal, the signal resulting from the beta dose was measured after the same period as that elapsed between ion irradiation and measurement (see step 5). It was thereby assumed that beta- and ion-induced signals fade at the same rate. Steps 2, 3, 7, and 8 were introduced to correct for any changes that might occur during the storage period such as loss of grains during handling, sensitivity change of PMT and optics or variations of the LED stimulation power. The “normalized

dose” was then calculated according to the following relation:

$$normalized\ dose = \frac{OSL_{ion}/(OSL_1^*D_{ion})}{OSL_{\beta}/(OSL_2^*D_{\beta})}$$

5.3. Results

The normalized doses for various ions and depths in regolith are plotted in Figs. 8 and 9. The ion doses at zero depth in regolith are known. The normalized dose at zero depth therefore equals the efficiency in luminescence production for the respective primary ion beams. For depths >0 cm the actual deposited dose varies with depth. The composition and energy of the radiation field change with depth due to absorption and scattering of the primary ion beam and the production of secondary particles. The intensity of the OSL signal measured at each depth, and with it the normalized dose, depend, therefore, on the absorbed dose as well as the LET of the particles encountered at that depth.

For 1 GeV protons the OSL signal shows a maximum at 10 cm depth, followed by a slow decrease. The maximum is caused by the build up of secondary particles (mainly secondary protons) and the concomitant loss of primary particles. The expected range of 1 GeV protons in regolith material is ~2m, however the range for the heavier particles is considerably less. Thus, the signals resulting from the heavier charged particles show an initial plateau before a sharp peak (the Bragg-peak) and a rapid drop-off to zero. This is most evident for 500 MeV/u Fe, whereas in other cases the peaks appear broadened due to the low density of measurement points. Jain et al. (2006) observed a Bragg peak also for 175 MeV protons. The penetration depth and the peak signal depend strongly on ion type and energy.

The efficiency, i.e. the normalized dose at zero depth, for the various ion beams and minerals is plotted against the LET (in water) in Fig. 10. The efficiency for beta and gamma radiation is assumed to be equal to 1. The efficiency

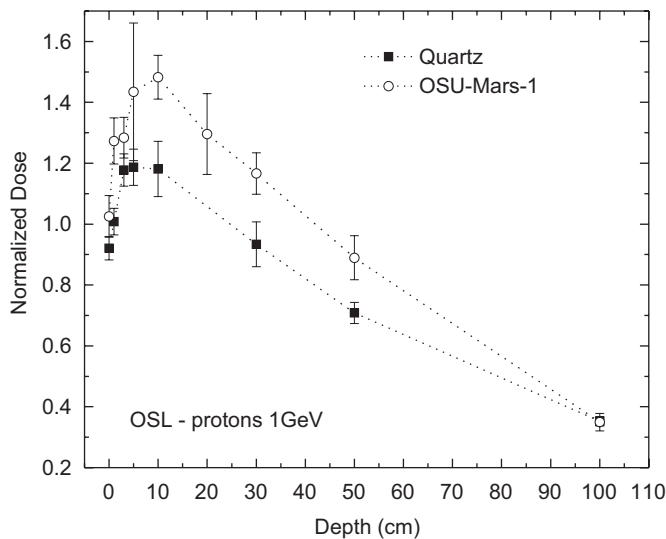


Fig. 8. Normalized dose deposited at various depths in regolith simulant, after exposure to 1 GeV protons. Lines are drawn to guide the eye but do not resemble the actual trend between measured points. Error bars result from the standard error of four aliquots.

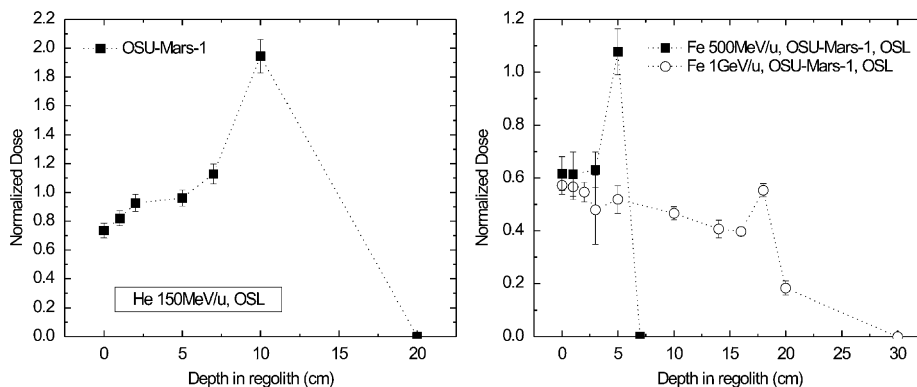


Fig. 9. Normalized dose deposited at various depths in the regolith simulant, after exposure to 150 MeV/u He ions (left), 1 GeV/u Fe (right, gray) and 500 MeV/u Fe ions (right, black). Lines are drawn to guide the eye. Error bars are the standard errors obtained from measurement of four aliquots.

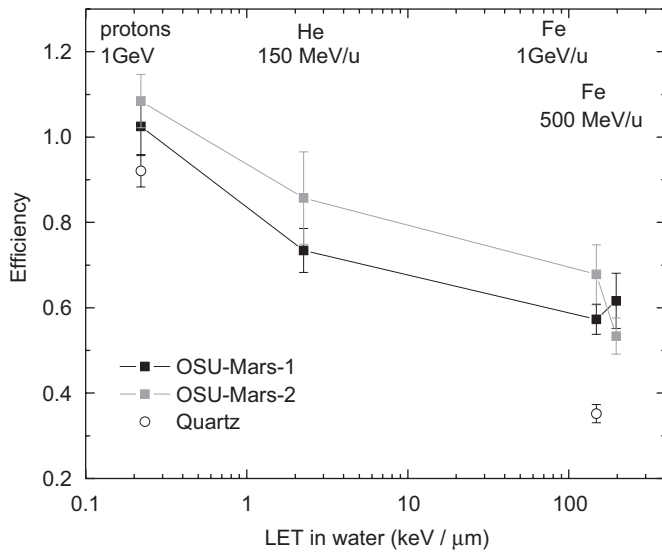


Fig. 10. Efficiency in OSL production of various ion beams for OSU Mars-1, -2 and quartz.

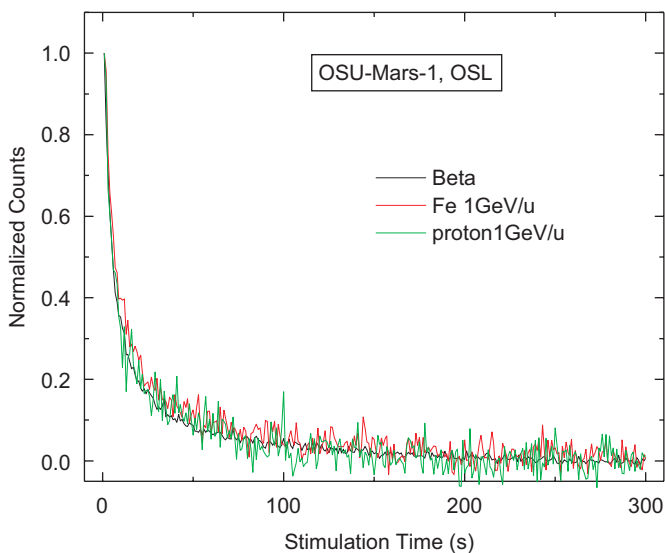


Fig. 11. Normalized OSL curves for OSU Mars-1, measured after irradiation with the indicated ions and the ^{90}Sr source.

decreases with increasing LET. It is smaller for quartz than for the mineral mixtures (see also Fig. 8).

Yukihara et al. (2004), using $\alpha\text{-Al}_2\text{O}_3\text{:C}$ dosimeters, found that particles with different LETs produce different shapes of OSL decay curves and that decay parameters could be found that were indicative of the radiation particle LET. Thus, LET information derived from the OSL decay curve could help to both identify the type of irradiation and to correct the absorbed radiation dose. The OSL-curve shapes of the minerals in the present study, however, do not change with LET and thus cannot be used as indicator for particle LET. As an example, the normalized OSL curves for OSU Mars-1, measured after irradiation with protons, Fe-ions and beta radiation are plotted in Fig. 11.

6. Discussion and conclusion

We used mixtures of plagioclase, clinopyroxene and potassium-rich glass, in various proportions to approximate the type of polymineralic samples that might be found on the martian surface. Experiments and simulations were carried out to investigate the effects of the many situational challenges encountered in the determination of the equivalent dose from martian samples as well as in the determination of the natural dose rate under martian conditions.

Modeling of radiation transport in the martian atmosphere suggested a more intense UV component than is found on Earth. Experiments with a Mars solar simulator indicate efficient bleaching of the OSL signals from the soil simulants. The results suggest efficient zeroing of the OSL signal for solar-exposed sediments on Mars and thus a satisfactory OSL-resetting criterion. OSL dose-recovery experiments, at Earth ambient temperatures using IR stimulation and post-IR blue stimulation, reveal that a viable SAR procedure for polymineralic samples is possible. Low-temperature measurements and simulations indicate that known doses delivered at low temperatures can be effectively estimated as long as the stimulation temperature is considerably greater than the highest temperature during the initial irradiation, i.e. in the case of Mars at least 80–100 °C.

A remaining significant issue for the estimation of the equivalent dose is anomalous fading. Initial experiments indicate that the fading is initially rapid, stabilizing after a few days. This issue will require further and detailed examination. However, if the observation is confirmed in later experiments, one may have a situation where the unstable component has already faded in any martian sediment sample that is extracted for OSL measurement. It is intended to characterize the fading properties of the regolith simulants and to determine an adjustment of the measurement procedure to correct the signal instability. The most likely and least energy consuming means is to allow time for fading after each calibration irradiation. Another possibility that we plan to investigate is the use of the red OSL emission signal that is less prone to fading.

The natural dose rate on Mars consists of two components. Radioactive nuclides play only a minor role in the near-surface deposits on Mars and currently available data from the Mars Odyssey Gamma-Ray Spectrometer (e.g. Boynton et al., 2004; Wänke et al., 2005) will be sufficient to determine the resulting dose rate background. The major contribution stems from cosmic and solar particle radiation. Both dose rate and composition of the radiation vary with depth, and various computer models exist to determine the radiation environment on the martian surface and in the martian regolith. One example is the HZETRN heavy ion code (Wilson et al., 1995; De Angelis et al., 2004), which allows for high charge and high energy transport, with energy deposition from both primary and secondary particles. It provides

particle energy spectra and dosimetric quantities at predefined positions in the material of interest. Using such techniques the radiation dose absorbed in the minerals at a defined burial depth can be estimated, as well as the composition of the cosmic-ray spectrum.

The identification of the most suitable code and depth-profiles of particle energy spectra and dosimetric quantities are, however, only one of the necessary steps towards the age determination. The experiments above demonstrate that even for the same administered dose, the OSL signal depends on the type and energy of the ions. It will therefore be necessary to determine efficiency-depth profiles for the relevant particles in the cosmic radiation. More accelerator-based experiments with a wide variety of ions, in particular protons, will be required. The results of these experiments can then be combined with the simulations to determine an “equivalent natural dose rate” at a given depth for age calculation. GCR and SEP spectra are dominated by the lower LET parts of the spectrum, to the extent that an estimated 95% of the dose will be deposited by these particles. As a result, the drop in efficiency with LET of the primary particles may only induce a small error. A bigger source of error will be the fact that the dose rate will not be constant over the lifetime of the buried sediment due to the slow burial of the sediment.

Assuming a lower measurable dose limit of 5 Gy (Kalchgruber et al., 2006) and a average surface dose rate of 100 mGy/yr (e.g. Saganti et al., 2004), the lower age limit can be expected to be few decades. With an upper measurable dose limit of 1500 Gy the upper age limit would be only 10,000 years and thus considerably lower than on Earth. It has to be taken into account, however, that the dose rate decreases rapidly with increasing burial depth. At 3–4 m depth and a background dose rate of 0.5 mGy/yr (Pavlov et al., 2002; see also McKeever et al., 2003) the upper age limit would be 3 Ma. Depending on the burial rate, the upper age limit is therefore expected to be in the region of several 10^5 years. Burial over a depth of 1 m will result in a dose rate difference of about 75% (see e.g. Dartnell et al., 2007) and burial models might have to be developed. In the worst case the age can be bracketed by calculating an age based on the surface dose rate, or the dose rate at the depth from which the sample is recovered. These ages will then vary by approximately a factor of 4. The significance of such a result would be quite limited in terrestrial applications. But, given the age range covered with luminescence dating, and the fact that ages smaller than at least 1 Myr cannot be resolved by crater counting, even such results will be a major improvement to current Mars dating techniques. Luminescence dating could nevertheless be used to prove that water was flowing on the martian surface in the recent past.

Acknowledgments

The project is funded by NASA (JPL Contract no. 1265427 under Grant NASA RTOP No. 344-36-55-19) and

a Research Initiation Grant from Oklahoma NASA EPSCoR. The authors want to thank Gabriel Sawakuchi for his support with the experiments at HIMAC and NSRL/BNL, and the staff of the NIRS HIMAC and the NSRL/BNL for their assistance in making the accelerator irradiations.

References

- Aitken, M.J., 1985. Thermoluminescence Dating. Academic Press, London.
- Aitken, M.J., 1998. An Introduction to Optical Dating. Oxford University Press, Oxford, UK.
- Albee, A.L., 2003. The unearthy landscapes of Mars. *Sci. Am.* 13, 34–44.
- Allen, C.C., Jager, K.M., Morris, R.V., Lindstrom, D.J., Lockwood, J.P., 1998. JSC Mars-1: a martian soil simulant. In: *Space '98, Proceedings of the American Society of Civil Engineers*, pp. 469–476.
- Armstrong, J.C., Leovy, C.B., 2005. Long-term wind erosion on Mars. *Icarus* 176 (1), 57–74.
- Auclair, M., Lamothe, M., Huot, S., 2003. Measurement of anomalous fading for feldspar IRSL using SAR. *Radiat. Meas.* 37, 487–492.
- Bailiff, I.K., Poolton, N.R.J., 1991. Studies of charge transfer mechanisms in feldspars. *Nucl. Tracks Radiat. Meas.* 18, 111–118.
- Baker, V.R., 2001. Water and the martian landscape. *Nature* 412, 228–236.
- Bandfield, J.L., 2002. Global mineral distribution on Mars. *J. Geophys. Res.-Planets* 107 (E6) Art. No. 5042 JUN 2002.
- Bandfield, J.L., Hamilton, V.E., Christensen, P.R., 2000. A global view of martian surface compositions from MGS-TES. *Science* 287, 1626–1630.
- Banerjee, D., Bøtter-Jensen, L., Murray, A.S., 2001. Retrospective dosimetry: estimation of the dose to quartz using the single-aliquot regenerative-dose protocol. *Appl. Radiat. Isot.* 52, 831–844.
- Banerjee, D., Blair, M.W., Sears, D.W.G., McKeever, S.W.S., 2002a. Dating martian meteorites: characterization of luminescence from a martian soil simulant and martian meteorites. In: *Proceedings of the 33rd Lunar and Planetary Science Conference*, Abstract #1561.
- Banerjee, D., Blair, M.W., Lepper, K., McKeever, S.W.S., 2002b. Optically stimulated luminescence signals of polymineral fine grains in the JSC Mars-1 soil simulant sample. *Radiat. Protect. Dosim.* 101, 321–326.
- Banerjee, D., Hildebrand, A.N., Murray-Wallace, C.V., Bourman, R.P., Brooke, B.P., Blair, M., 2003. New quartz OSL ages from the stranded beach dune sequence in south-east Australia. *Quaternary Sci. Rev.* 22, 1019–1025.
- Barbouti, A., Rastin, B., 1983. A study of the absolute intensity of muons at sea level and under various thicknesses of absorber. *J. Phys. G: Nucl. Phys.* 9, 1577–1595.
- Benton, E.R., Benton, E.V., 2001. Space radiation dosimetry in low-earth orbit and beyond. *Nucl. Instrum. Methods B* 184, 255–294.
- Blair, M.W., Yukihara, E.G., Kalchgruber, R., McKeever, S.W.S., 2003. In-situ dating on Mars: procedure and characterization of luminescence from a Martian soil simulant and Martian meteorites. In: *Proceedings of the Sixth International Conference on Mars*, Abstract #3201.
- Blair, M.W., Yukihara, E.G., McKeever, S.W.S., 2005. Experiences with single-aliquot OSL procedures using coarse-grain feldspars. *Radiat. Meas.* 39 (4), 361–374.
- Blair, M.W., Kalchgruber, R., McKeever, S.W.S., 2006a. Progress towards a polymineral single-aliquot OSL dating procedure. *Radiat. Protect. Dosim.* 119 (1–4), 450–453.
- Blair, M.W., Yukihara, E.G., McKeever, S.W.S., 2006b. A system to irradiate and measure luminescence at low temperatures. *Radiat. Protect. Dosim.* 119 (1–4), 454–457.

- Bøtter-Jensen, L., Bulur, E., Døller, G.A.T., Murray, A.S., 2000. Advances in luminescence instrument systems. *Radiat. Meas.* 32, 523–528.
- Boynton, W.V., Feldman, W.C., Mitrofanov, I.G., Evans, L.G., Reedy, R.C., Squyres, S.W., Starr, R., Trombka, J.I., D'Uston, C., Arnold, J.R., Englert, P.A.J., Metzger, A.E., Wänke, H., Brückner, J., Drake, D.M., Shinohara, C., Fellows, C., Hamara, D.K., Harshman, K., Kerry, K., Turner, C., Ward, M., Barthe, H., Fuller, K.R., Storms, S.A., Thornton, G.W., Longmire, J.L., Litvak, M.L., Ton'chev, A.K., 2004. The Mars Odyssey gamma-ray spectrometer instrument suite. *Space Sci. Rev.* 110 (1–2), 37–83.
- Burr, D.M., McEwen, A.S., 2002. Recent aqueous floods from the Cerberus Fossae, Mars. *Geophys. Res. Lett.* 29 (13), 1–4.
- Byrne, S., Murray, B.C., 2002. North polar stratigraphy and the paleo-erg of Mars. *J. Geophys. Res.* 107 (11), 1–12.
- Cabrol, N.A., Grin, E.A., 2002a. The recent Mars global warming (MGW) and/or south pole advance (SPA) hypothesis: global geological evidence and reasons why gullies might still be forming today. In: 33rd Lunar and Planetary Science Conference, Abstract #1058.
- Cabrol, N.A., Grin, E.A., 2002b. Astrobiological implications of modern glaciers and surface ice on Mars. In: Second Astrobiology Conference, NASA Ames Research Center.
- Cabrol, N.A., Grin, E.A., Dohm, J.M., 2001. From gullies to glaciers: a morphological continuum supporting a recent climate change on Mars. In: American Geophysical Union Abstracts with Programs, vol. 82(47), San Francisco, p. F694.
- Dartnell, L.R., Desorgher, L., Ward, J.M., Coates, A.J., 2007. Modelling the surface and subsurface Martian radiation environment: implications for astrobiology. *Geophys. Res. Lett.* 34, L02207.
- De Angelis, G., Cloudsley, M.S., Singletary, R.C., Wilson, J.W., 2004. A new Mars radiation environment model with visualization. *Adv. Space Res.* 34 (6), 1395–1403.
- Deo, S., Kalchgruber, R., Mayer, B., 2005. Radiative transfer calculations for the atmosphere of Mars in the 200–900 nm range. In: 36th Lunar and Planetary Science Conference, Abstract #1029.
- Doran, P.T., Clifford, S.M., Forman, S.L., Nyquist, L., Papanastassiou, D.A., Stewart, B.W., Sturchio, N.C., Swindle, T.D., Cerling, T., Kargel, J., McDonald, G., Nishiizumi, K., Poreda, R., Rice, J.W., Tanaka, K., 2004. Mars chronology: assessing techniques for quantifying surficial processes. *Earth Sci. Rev.* 67, 313–333.
- Edgett, K.S., Malin, M.C., 2000. New views of Mars eolian activity, materials, and surface properties: three vignettes from the Mars Global Surveyor Mars Orbiter Camera. *J. Geophys. Res.* 105, 1623–1650.
- Fattahi, M., Stokes, S., 2003. Red luminescence from potassium feldspars for dating applications: a study of some properties relevant for dating. *Radiat. Meas.* 37, 647–660.
- Fishbaugh, K., Head, J.W., Pratt, S., 2000. South Polar chasmata: analysis of MOLA data and evidence for basal melting and ponding in the Prometheus Basin. In: Proceedings of the Lunar Planetary Science Conference, vol. 31, Abstract #1206.
- Gilmore, M.S., Phillips, E.L., 2002. Role of aquicludes in formation of martian gullies. *Geology* 30, 1107–1110.
- Greeley, R., 1992. Saltation impact as a means of raising dust on Mars. *Planet. Space Sci.* 50, 151–155.
- Grotzinger, J.P., Arvidson, R.E., Bell III, J.F., Calvin, W., Clark, B.C., Fike, D.A., Golombek, M., Greeley, R., Haldemann, A., Herkenhoff, K.E., Jolliff, B.L., Knoll, A.H., Malin, M., McLennan, S.M., Parker, T., Soderblom, L., Sohl-Dickstein, J.N., Squyres, S.W., Tosca, N.J., Watters, W.A., 2005. Stratigraphy and sedimentology of a dry to wet eolian depositional system, burns formation, Meridiani Planum, Mars. *Earth Planet. Sci. Lett.* 240, 11–72.
- Hartmann, W.K., 2005. Martian cratering 8: isochron refinement and the chronology of Mars. *Icarus* 174, 294–320.
- Hartmann, W.K., Neukum, G., 2001. Cratering chronology and the evolution of Mars. *Space Sci. Rev.* 96 (1–4), 165–194.
- Head, J.W., Mustard, J.F., Kreslavsky, M.A., Milliken, R.E., Marchant, D.R., 2003. Recent ice ages on Mars. *Nature* 426, 797–802.
- Huntley, D.J., Lamothe, M., 2001. Ubiquity of anomalous fading in K-feldspars and the measurement and correction for it in optical dating. *Can. J. Earth Sci.* 38, 1093–1106.
- Jain, M., Andersen, C.E., Bøtter-Jensen, L., Murray, A.S., Haack, H., Bridges, J.C., 2006. Luminescence dating on Mars: OSL characteristics of Martian analogue materials and GCR dosimetry. *Radiat. Meas.* 41, 755–761.
- Kalchgruber, R., Blair, M.W., McKeever, S.W.S., 2006. Dose recovery with plagioclase and pyroxene samples as surrogates for martian surface sediments. *Radiat. Meas.* 41 (7–8), 762–767.
- Kieffer, H.H., Jakosky, B.M., Snyder, C.W., 1992. The planet Mars: from antiquity to present. In: Kieffer, H.H., Jakosky, B.M., Snyder, C.W., Mathews, M.S. (Eds.), Mars. University of Arizona Press, Tucson, pp. 1–33.
- Laskar, J., Levrard, B., Mustard, J., 2002. Orbital forcing of the Martian polar layered deposits. *Nature* 419 (6905), 375–377.
- Lepper, K., McKeever, S.W.S., 2000. Characterization of fundamental luminescence properties of the Mars soil simulant JSC Mars-1 and their relevance to absolute dating of martian sediments. *Icarus* 144, 295–301.
- Madsen, A.T., Murray, A.S., Andersen, T.J., Pejrup, M., Breuning-Madsen, H., 2005. Optically stimulated luminescence dating of young estuarine sediments: a comparison with ^{210}Pb and ^{137}Cs dating. *Mar. Geol.* 214, 251–268.
- Mahaney, W.C., Miyamoto, H., Dohm, J.M., Baker, V.R., Cabrol, N.A., Grind, E.A., Berman, D.C., 2007. Rock glaciers on Mars: Earth-based clues to Mars' recent paleoclimatic history. *Planet. Space Sci.* 55, 181–192.
- Malin, M.C., Edgett, K.S., 2000. Sedimentary rocks of early Mars. *Science* 290, 1927–1937.
- Malin, M.C., Edgett, K.S., 2003. Evidence for persistent flow and aqueous sedimentation on early Mars. *Science* 302, 1931–1934.
- Malin, M.C., Caplinger, M.A., Davis, S.R., 2001. Observational evidence for an active surface reservoir of solid carbon dioxide on Mars. *Science* 294, 2146–2148.
- Mangold, N., Ansan, V., 2006. Detailed study of an hydrological system of valleys, a delta and lakes in the Southwest Thaumasia region, Mars. *Icarus* 180 (1), 75–87.
- Márquez, A., Fernández, C., Anguita, F., Farelo, A., Anguita, J., de la Casa, M.-A., 2004. New evidence for a volcanically, tectonically, and climatically active Mars. *Icarus* 172, 573–581.
- Mayer, B., Kylling, A., 2005. Technical note: the libRadtran software package for radiative transfer calculations—description and examples of use. *Atmos. Chem. Phys.* 5, 1855–1877.
- McEwen, A.S., Malin, M.C., Carr, M.H., Hartmann, W.K., 1999. Voluminous volcanism on early Mars revealed in Valles Marineris. *Nature* 397, 584–586.
- McKeever, S.W.S., Banerjee, D., Blair, M.W., Clifford, S.M., Cloudsley, M.S., Kim, S.S., Lamothe, M., Lepper, K., Leuschen, M., McKeever, K.J., Prather, M., Rowland, A., Reust, D., Sears, D.W.G., Wilson, J.W., 2003. Concepts and approaches to in-situ luminescence dating of martian sediments. *Radiat. Meas.* 37, 527–534.
- McKeever, S.W.S., Kalchgruber, R., Blair, M.W., Deo, S., 2006. Development of methods for in-situ dating of martian sediments. *Radiat. Meas.* 41 (7–8), 750–754.
- Milam, K.A., McSween, H.Y., Hamilton, V.E., Moersch, J.M., Christensen, P.R., 2004. Accuracy of plagioclase compositions from laboratory and Mars spacecraft thermal emission spectra. *J. Geophys. Res.-Planets* 109 (E4) (Art. No. E04001 APR 7 2004).
- Milkovich, S.M., Head III, J.W., 2005. North polar cap of Mars: polar layered deposit characterization and identification of a fundamental climate signal. *J. Geophys. Res.* 110, E01005.
- Murray, A.S., Wintle, A.G., 2000. Luminescence dating of quartz using an improved single-aliquot regenerative-dose protocol. *Radiat. Meas.* 32, 57–73.
- Mustard, J.F., Cooper, C.D., Rifkin, M.K., 2001. Evidence for recent climate change on Mars from the identification of youthful near-surface ground ice. *Nature* 412, 411–414.

- Olley, J.M., De Deckker, P., Roberts, R.G., Fifield, L.K., Yoshida, H., Hancock, G., 2004. Optical dating of deep-sea sediments using single grains of quartz: a comparison with radiocarbon. *Sediment. Geol.* 169, 175–189.
- Ori, G.G., Marinangeli, L., Baliva, A., 2000. Terraces and Gilbert-type deltas in crater lakes in Ismenius Lacus and Memnonia, Mars. *J. Geophys. Res.* 105 (E7), 17629–17641.
- Patel, M.R., Zarnecki, J.C., Catling, D.C., 2002. Ultraviolet radiation on the surface of Mars and the Beagle 2 UV sensor. *Planet. Space Sci.* 50, 915–927.
- Pavlov, A.K., Blinov, A.V., Konstantinov, A.N., 2002. Sterilization of Martian surface by cosmic radiation. *Planet. Space Sci.* 50, 669–673.
- Poolton, N.R.J., Mauz, B., Lang, A., Jain, M., Malins, A.E.R., 2006. Optical excitation processes in the near band-edge region of KAlSi_3O_8 and $\text{NaAlSi}_3\text{O}_8$ feldspar. *Radiat. Meas.* 41, 542–548.
- Prescott, J.R., Stephan, L.G., 1982. The contribution of cosmic radiation to the environmental dose for thermoluminescence dating. *PACT* 6, 17–25.
- Roberts, H.M., Wintle, A.G., 2003. Luminescence sensitivity changes in of polymineral fine-grains during IRSL and [post-IR] OSL measurements. *Radiat. Meas.* 37, 661–671.
- Saganti, P.B., Cucinotta, F.A., Wilson, J.W., Simonsen, L.C., 2004. Radiation climate map for analyzing risks to astronauts on the Mars surface from galactic cosmic rays. *Space Science Reviews* 110, 143–156.
- Shubert, G.C., Solomon, S.C., Turcotte, D.L., Drake, M.J., Sleep, N.H., 1992. Origin and thermal evolution of Mars. In: Kieffer, H.H., Jakosky, B.M., Snyder, C.W., Matthews, M.S. (Eds.), *Mars*. University of Arizona Press, Tucson, pp. 147–183.
- Squyres, S.W., Knoll, A.H., 2005. Sedimentary rocks at Meridiani Planum: origin, diagenesis, and implications for life on Mars. *Earth Planet. Sci. Lett.* 240, 1–10.
- Thomas, P.C., Malin, M.C., James, P.B., Cantor, B.A., Williams, R.M.E., Gierasch, J., 2005. South polar residual cap of Mars: features, stratigraphy, and changes. *Icarus* 174, 535–559.
- Wallinga, J., Murray, A.S., Boettger-Jensen, L., 2002. Measurement of the dose in quartz in the presence of feldspar contamination. *Radiat. Protect. Dosim.* 101, 367–370.
- Wänke, H., Boynton, W.V., Brückner, J., Dreibus, G., Taylor, G.J., Evans, L., James, B., Keller, J., Kerry, K., Starr, R., GRS Team, 2005. Sulfuric acid all over early Mars? In: 36th Lunar and Planetary Science Conference, Abstract #1389.
- Watanuki, T., Murray, A.S., Tsukamoto, S., 2005. Quartz and polymineral luminescence dating of Japanese loess over the last 0.6 Ma: comparison with an independent chronology. *Earth Planet. Sci. Lett.* 240, 774–789.
- Williams, J., Paige, D.A., Manning, C.E., 2003. Layering in the wall rock of Valles Marineris: intrusive and extrusive magmatism. *Geophys. Res. Lett.* 30 (12), 25.
- Wilson, J.W., Badavi, F.F., Cucinotta, F.A., Shinn, J.L., Badhwar, G.D., Silberberg, R., Tsao, C.H., Townsend, L.W., Tripathi, R.K., 1995. HZETRN: description of a free-space ion and nucleon transport and shielding computer program. NASA TP-3495.
- Wintle, A.G., 1997. Luminescence dating: laboratory procedures and protocols. *Radiat. Meas.* 27, 769–817.
- Wintle, A.G., Murray, A.S., 2006. A review of quartz optically stimulated luminescence characteristics and their relevance in single-aliquot regeneration dating protocols. *Radiat. Meas.* 41, 369–391.
- Wolff, M.J., Clancy, R.T., 2003. Constraints on the size of Martian aerosols from thermal emission spectrometer observations. *J. Geophys. Res. Planets* 108 (E9).
- Yukihara, E.G., Gaza, R., McKeever, S.W.S., Soares, C.G., 2004. Optically stimulated luminescence and thermoluminescence efficiencies for high-energy heavy charged particle irradiation in Al_2O_3 : C. *Radiat. Meas.* 38, 59–70.